Charge Carrier Separation in Solar Cells

Uli Würfel, Andres Cuevas, *Fellow, IEEE*, and Peter Würfel

***Abstract*—The selective transport of electrons and holes to the two terminals of a solar cell is often attributed to an electric field, although well-known physics states that they are driven by gradients of quasi-Fermi energies. However, in an illuminated semiconductor, these forces are not selective, and they drive both charge carriers toward both contacts. This paper shows that the necessary selectivity is achieved by differences in the conductivities of electrons and holes in two distinct regions of the device, which, for one charge carrier, allows transport to one contact and block transport to the other contact.**

To clarify the physics, we perform numerical simulations of three different solar cell structures with asymmetric carrier conductivities. Two of them achieve the ideal conversion efficiency limit, despite the fact that the charge carriers flow *against* an internal electric field, proving that the latter cannot explain carrier separation. A third, i.e., conceptual structure, has no electric field at all but still works ideally as a solar cell. In conclusion, the different conductivities of electrons and holes in two regions of the device can be identified as the essential ingredient for charge carrier separation in solar cells, regardless of the existence of an electric field.

***Index Terms*—Charge carriers, photovoltaic cells, radiative recombination, semiconductor device doping, semiconductor device modeling, semiconductor-metal interfaces.**

I. Introduction

IN A POPULAR view, a p-n junction is seen as essential for solar cell operation, and the electric field present in the dark between the space charge layers of the p- and n-type parts of the junction is thought to be the driving force for the electric current once the solar cell is illuminated. For many, it is inconceivable that solar cells may work without a preexisting electric field and the consequent built-in electrical potential difference between the p-type and n-type regions of the junction. According to that mentality, there cannot be charge carrier separation without an electric field, and the movement of the carriers against an electric field in the operation of a solar cell is unimaginable. This type of thinking is also reflected by the unphysical terminology used by most solar cell researchers [1].

Despite being broadly disseminated, such interpretation is incorrect. To start with, it should be realized that for the electric field, which is present in the dark, to be able to drive the charge carriers toward their terminals, it would have to do work on them, due to their finite conductivity. However, there is no energy source behind this field that would allow work to be done, since it is a consequence of thermal equilibrium. Second, solar cell configurations exist, some of which will be discussed here, where there is no electric field at the operating point of the solar cell, or where the charge carriers even flow in a direction opposite to the electric field.

In this paper, we present an alternative explanation of solar cell operation that is straightforward and not in conflict with the laws of physics. It is based on the fact that the driving forces for charge carrier transport in a semiconductor are the gradients of the quasi-Fermi energies. These, however, are not sufficient to cause selective carrier transport. As will be shown in the following, the separation and selective transport of electrons and holes to different terminals is fundamentally based on establishing different conductivities for each of them in different regions of the device. The conductivity should be large for electrons and small for holes at the electron contact and *vice versa* at the hole contact.

To demonstrate the general validity of our approach, we present in Section III detailed numerical simulations of three different solar cell structures. For one of them, the electric potential difference in the dark is larger than the open-circuit voltage under illumination, as it is commonly expected, but for the other two it is not. One of the devices analysed does not even have any electric potential difference in the dark. As will be shown, the physical principles reviewed here explain the behavior of all solar cell structures, independent of the existence or not, of an electrical potential difference.

Before discussing the results of the numerical simulations for each structure, we summarize briefly which are the forces that act upon electrons and holes and how selective transport toward different contacts can be achieved.

II. Summary of the Underlying Physics

A. Forces Acting on Electrons and Holes

In a semiconductor, electrons and holes are exposed simultaneously to different forces. Two of them are important for solar cell operation, one is the electric force and the other "generalized" force is related to the gradient of their concentration. The following presentation follows the derivations in [2].

1) If the electric field E is the only force, then the charge current of particles k (electrons e or holes h) with a charge of $z_k e$ (where e is the elementary charge) and a concentration of n_k is given by

$$j_{\mathrm{f},k} = \mathrm{e} n_k \mu_k E = \sigma_k E = -\frac{\sigma_k}{z_k \mathrm{e}} \mathrm{grad}(z_k \mathrm{e}\varphi) \quad (1)$$

where μ_k is the mobility of the particles, and σ_k is their electrical conductivity. φ is the electric potential, and the electric force acting on the particles is $-\mathrm{grad}(z_k \mathrm{e}\varphi)$.

Manuscript received July 10, 2014; revised September 12, 2014; accepted October 12, 2014. Date of publication November 20, 2014; date of current version December 18, 2014.

U. Würfel is with the Fraunhofer Institute for Solar Energy Systems, 79110 Freiburg, Germany, and also with the Materials Research Center, University of Freiburg, 79104 Freiburg, Germany (e-mail: uli.wuerfel@ise.fraunhofer.de).

A. Cuevas is with the Research School of Engineering, Australian National University, Canberra ACT 0200, Australia (e-mail: andres.cuevas@anu.edu.au).

P. Würfel is with the Karlsruhe Institute of Technology, 76131 Karlsruhe, Germany (e-mail: peter.wuerfel@partner.kit.edu).

Digital Object Identifier 10.1109/JPHOTOV.2014.2363550

2) If there is only a concentration gradient of particles k present and no electric field, their charge current is given by Fick's law

$$j_{\mathrm{d},k} = z_k \mathrm{e}(-D_k \mathrm{grad}\, n_k) = -z_k \mathrm{e} n_k D_k \frac{\mathrm{grad}\, n_k}{n_k} = -\frac{\sigma_k}{z_k \mathrm{e}} \mathrm{grad}\, \Phi_{\mathrm{chem,k}}. \quad (2)$$

For this relation, we have used the chemical potential $\Phi_{\mathrm{chem},k} = \Phi_{\mathrm{chem},k,0} + \mathrm{k}T \ln(\frac{n_k}{N_0})$ of particles k with a standard value of the chemical potential $\Phi_{\mathrm{chem},k,0}$ at a standard concentration N_0, and Einstein's relation $D_k = \mu_k \mathrm{k}T/e$ between the diffusion coefficient D_k and the mobility μ_k. The chemical force acting on the particles and causing diffusion is $-\mathrm{grad}\ \Phi_{\mathrm{chem},k}$.

If both the electrical force and the chemical force are present simultaneously, they must first be added to give the resulting force, which then causes the particles to move and contribute to a current. This resulting force is $-\mathrm{grad}(\Phi_{\mathrm{chem},k} + z_k \mathrm{e}\varphi) = -\mathrm{grad}\ \eta_k$, where η_k is the electrochemical potential of particles k. Mathematically, it makes no difference if first the two currents (1) and (2) are calculated separately and then added to give the total current, or if first the driving forces are added and the total current is calculated, but care has to be taken, as the two current components in the first case lack a real physical meaning; they do not exist, only the total current originating from the total driving force is a real physical quantity.

In a final step, we make use of the identity between the electrochemical potential $\eta_{\mathrm{e}} = \varepsilon_{\mathrm{FC}}$ of the electrons in the conduction band and their (quasi-) Fermi energy $\varepsilon_{\mathrm{FC}}$, which describes the occupation of states in the conduction band. In the same way, the electrochemical potential of the holes $\eta_{\mathrm{h}} = -\varepsilon_{\mathrm{FV}}$, where $\varepsilon_{\mathrm{FV}}$ is the (quasi-) Fermi energy, which describes the occupation of states in the valence band.

In conclusion, the charge current of electrons with $z_e = -1$ is in all cases, whether there is an electric field or not, or a concentration gradient or not, given by

$$j_{\mathrm{e}} = \frac{\sigma_{\mathrm{e}}}{\mathrm{e}} \mathrm{grad}\, \eta_{\mathrm{e}} = \frac{\sigma_{\mathrm{e}}}{\mathrm{e}} \mathrm{grad}\, \varepsilon_{\mathrm{FC}}. \quad (3)$$

The charge current of holes with $z_h = 1$ is

$$j_{\mathrm{h}} = -\frac{\sigma_{\mathrm{h}}}{\mathrm{e}} \mathrm{grad}\, \eta_{\mathrm{h}} = \frac{\sigma_{\mathrm{h}}}{\mathrm{e}} \mathrm{grad}\, \varepsilon_{\mathrm{FV}}. \quad (4)$$

Equations (3) and (4) describe the only real charge currents of electrons and holes in semiconductors in steady state. The simultaneous and independent existence of field currents and diffusion currents is a myth.

With a simple, but perhaps less-familiar, argument, particles can only move in a direction in which their free energy is decreasing, thereby allowing entropy to be generated. Since the electrochemical potential is the free energy of charged particles at constant temperature and constant volume, (3) and (4) follow directly without explicit use of fields and concentration gradients.

B. Separation of Electrons and Holes in Solar Cells

In order to generate an electrical current in a solar cell, electrons and holes have to move toward different contacts. This movement can only be caused by the forces in (3) and (4): the gradients of the Fermi energies. It would be nice to be able to establish a force that drives electrons and holes in different directions, in the way that an electric field would do. But the real forces acting on the electrons and the holes are the gradients of the quasi-Fermi energies and these forces cannot be "*a priori*" implemented in such a way that they are directed for electrons toward one contact and for holes toward the other contact, except by applying an external voltage. Selective carrier transport in a solar cell cannot, therefore, be based on the driving forces alone, but requires another property. It is evident from (3) and (4) that selective transport can only result from different conductivities of electrons and holes on the way toward "their" contacts.

From the preceding discussion, a general design rule for all solar cells can be derived. In the vicinity of the contact toward which we want the electrons to flow, but not the holes, the electron conductivity must be large and the hole conductivity must be small. This contact is the "electron contact," which is the negative terminal of a solar cell. By the same reasoning, the hole conductivity must be large and the electron conductivity must be small in the vicinity of the "hole contact," which is the positive terminal of a solar cell.

This general design rule explains why a p-n junction works as a solar cell. A large electron conductivity and a small hole conductivity are provided by the n-type doping near the electron contact, which creates a high concentration of electrons and a low concentration of holes. *Vice versa*, large hole and small electron conductivities are provided by the p-type doping near the hole contact. The fact that there is a junction between the n- and p-type materials with a built-in electric field is irrelevant for charge carrier separation. It is merely a consequence of having used doping to achieve the aforementioned difference in conductivities of electrons and holes near the contacts. As we shall confirm below through numerical simulation, it is possible to conceive solar cells based exclusively on differential conductivities and where there are no preexisting electric fields. Selective conductivities are in fact only necessary in front of the contacts to prevent electrons (holes) to reach the hole (electron) contact. Sufficiently selective conductivities should fulfil the following conditions.

1) The electron (hole) current toward the electron (hole) contact should not produce a voltage drop of more than a few millivolts over the thickness of the solar cell in order to ensure a good fill factor.
2) The hole (electron) current toward the electron (hole) contact should be negligible, even in the presence of a large driving force in close vicinity of the contact.

III. Numerical Simulation Conditions

We have investigated with numerical simulations several different solar cell structures, three of which are presented in Section IV. Each of them has been designed according to the general design rule derived, i.e., ensuring large electron and small

hole conductivities near the electron contact and *vice versa* near the hole contact. It is not intended that all these structures represent realistic implementations of solar cells but that they serve to demonstrate the physical principles of solar cell operation and to unveil the real role of the electric field.

All the simulated structures comprise a 10-μm-thick absorber with a band gap of 1.34 eV, the optimal band gap for the AM 1.5G solar spectrum [3]–[5]. In the calculations, a uniform generation rate is created by homogeneously distributing the full absorption of all incident photons with energies greater than 1.34 eV from the AM1.5G spectrum and the surrounding 300 K radiation over the thickness d of the absorber. A maximum short-circuit current density of 35 mA/cm^2 results, if all generated electrons reach the electron contact and all generated holes the hole contact. The current density is given by

$$j = \int_0^d \mathrm{e}(R - G)\mathrm{d}x \tag{5}$$

where d is the thickness of the absorber and where the generation rate of electron–hole pairs $G = G_0 + \Delta G$ consists of the full absorption of photons with energy greater than 1.34 eV from the surrounding 300 K radiation G_0 and from the AM 1.5G spectrum ΔG. The radiative recombination rate is

$$R = k_\mathrm{r} n_\mathrm{e} n_\mathrm{h} = k_\mathrm{r} n_\mathrm{i}^2 \exp\left(\frac{\varepsilon_\mathrm{FC} - \varepsilon_\mathrm{FV}}{\mathrm{k}T}\right) \tag{6}$$

where n_i the intrinsic charge carrier density.

The recombination coefficient k_r is found by adjusting the recombination rate in the dark R_0 to the dark generation rate G_0:

$$R_0 = k_\mathrm{r} n_\mathrm{i}^2 = G_0. \tag{7}$$

In addition to radiative recombination, surface recombination at the electrodes is taken into account. Auger recombination and any recombination related to defects are neglected for the sake of simplicity. Nevertheless, taking them into account would not alter our general conclusions.

The contacts are assumed to cover the whole front and back surface of the semiconductor. As a consequence, if the derived design rule is not well realized in a given solar cell structure, i.e., if electrons and holes arrive at the same metal electrode, their surface recombination will reduce voltage and current of that solar cell structure. The recombination rate at the contacts may even be larger than in real solar cells, where the metal electrodes do not cover the whole surface in order to reduce shadowing losses and keep surface recombination as small as possible.

As an upper limit, under open-circuit conditions and if no other recombination mechanism is present in the absorber than radiative recombination, the aforementioned conditions result in a difference of the quasi-Fermi energies of $\varepsilon_\mathrm{FC} - \varepsilon_\mathrm{FV} = 1082\ \mathrm{meV}$ due to $R = G \rightarrow k_\mathrm{r} n_\mathrm{e} n_\mathrm{h} = G_0 + \Delta G$ and $\varepsilon_\mathrm{FC} - \varepsilon_\mathrm{FV} = \varepsilon_\mathrm{G} - \mathrm{k_B} T \ln(N_\mathrm{C} N_\mathrm{V}/n_\mathrm{e} n_\mathrm{h})$. This corresponds to the maximum value of the open-circuit voltage V_OC that can be achieved with this absorber and with this generation rate in any kind of single band gap solar cell structure. A solar cell in which electrons and holes recombine only radiatively is described by the Shockley–Queisser formalism [6]. The Shockley–Queisser limit for the band gap and generation rate specified above is given in Table I.

TABLE I
PHOTOVOLTAIC PARAMETERS ACCORDING TO THE SHOCKLEY–QUEISSER LIMIT FOR A SINGLE BAND GAP ABSORBER SOLAR CELL WITH A BAND GAP OF 1.34 eV UNDER ILLUMINATION WITH THE AM1.5G SPECTRUM

$J_\mathrm{SC}/\mathrm{mA cm^{-2}}$	$V_\mathrm{OC}/\mathrm{mV}$	FF/%	η/%	$J_\mathrm{MPP}/\mathrm{mA cm^{-2}}$	$V_\mathrm{MPP}/\mathrm{mV}$
35.0	1082	88.9	33.7	34.1	987

We have modeled three different solar cell structures. They differ from the ideal Shockley–Queisser limit by the fact that we implement a mechanism for carrier separation and we take the recombination at the electrode surfaces into account. Therefore, this study is basically an investigation of how well different structures can serve as an ideal solar cell by providing selective transport and thereby avoiding surface recombination at the electrodes.

All calculations were performed with the semiconductor device simulator Sentaurus TCAD from Synopsys [7]. A finite volume method is used to solve, self-consistently, the differential equations for drift and diffusion with the Poisson equation. Fermi statistics is used for electrons and holes. The contacts are characterized by their work functions and the surface recombination velocities of electrons and holes. The electron contact is always located at $x = 0$ and the hole contact at $x = 10$ μm. All contacts are full-area Ohmic contacts characterized by a work function equal to the work function of the adjacent semiconductor. In the case of a doped semiconductor, we assume full ionization of the dopants, i.e., for each donor (acceptor) atom, there is one additional electron (hole) in the conduction (valence) band. All parameters of the absorber in all the solar cell structures, together with their standard values are listed in Table II.

IV. EXEMPLARY SOLAR CELL DEVICE IMPLEMENTATIONS

We have selected three exemplary implementations of the general design rule stated in Section II-B. The first is based on controlling the carrier conductivity via doping, the second by using a higher bandgap material to create selective contacts, and the third is based on assuming strongly asymmetric mobilities for each type of carrier.

A. p-n-Homojunction Solar Cell

The requirements for selective conduction are most simply realised by a p-n homojunction. We implement it by dividing the 10-μm-thick absorber into a 5-μm-thick layer doped with a donor density of $n_\mathrm{D} = 10^{17}\ \mathrm{cm^{-3}}$ and another 5-μm-thick layer doped with an acceptor density of $n_\mathrm{A} = 10^{17}\ \mathrm{cm^{-3}}$, i.e., the junction is located in the middle of the device. Full-area Ohmic metal contacts are applied to both sides.

The energy band diagram in the dark (see Fig. 1) shows that there is only one Fermi-distribution for both the conduction and valence bands, with only one Fermi-energy ε_F. The gradient of

TABLE II
STANDARD PARAMETER SET FOR THE NUMERICAL SIMULATIONS

Symbol	Quantity	Standard value
χ_{e}	Electron affinity of absorber	-4.0 eV
ε_{G}	Band gap of absorber	1.34 eV
$N_{\mathrm{C,V}}$	Effective density of states of the conduction and valence band	2.51×10^{19} cm^{-3}
ΔG	Generation rate in absorber	2.18×10^{20} cm^{-3}s^{-1}
k_{r}	Radiative recombination coefficient in absorber	7.57×10^{-15} cm^{3}s^{-1}
$\mu_{\mathrm{e,h}}$	Electron and hole mobility in absorber	100 cm^2(Vs)$^{-1}$
T	Temperature	300 K
d	Thickness of absorber	10 μm
v_{sr}	Surface recombination velocity at the contacts	10^{12} cm s^{-1}
n_{i}	Intrinsic carrier concentration in absorber	1.39×10^{8} cm^{-3}

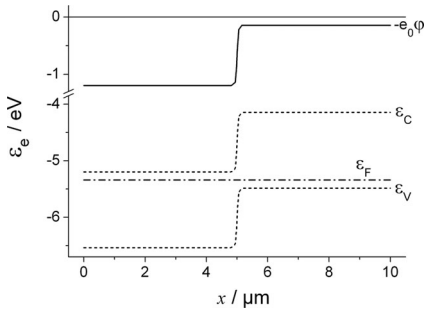

Fig. 1. Energy diagram for the p-n homojunction in the dark without applied voltage. The electron contact is located at $x = 0$ and the hole contact at $x = 10$ μm.

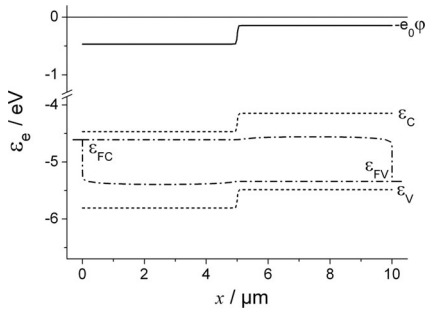

Fig. 2. Energy diagram for the p-n homojunction under illumination at the MPP, with $V_{\mathrm{MPP}} = 730$ mV and $J_{\mathrm{MPP}} = 17.1$ mA/cm^2. The electron contact is located at $x = 0$ and the hole contact at $x = 10$ μm. The voltage is the difference between the single Fermi-energies in the electron contact (left) and the hole contact (right), which is depicted as bold horizontal lines.

ε_{F} must be zero, since there must be no current in the dark without applied voltage. From this condition, it follows that there is a difference of the electric potential values φ between the p-side and the n-side of the p-n junction. This potential difference is usually called the "built-in voltage," which is $V_{\mathrm{bi}} = 1054$ mV in this case. In other words, the abrupt change of the electron and hole concentrations from the p-side to the n-side causes a large gradient of the chemical potential, according to (2). As a side effect, an electric force is established so that the total driving force is exactly zero. The corresponding "built-in" electric field is directed from the n-side toward the p-side (from the left toward the right in Fig. 1). Such direction is consistent with electrons moving toward the left and holes toward the right, leading to the common belief that the electric field is responsible for carrier separation in a solar cell, but of course, in equilibrium, there is no carrier separation and no separate drift and diffusion current components. Clearly, an explanation of solar cell operation under excitation cannot just be based on a partial component of the total driving force in equilibrium conditions.

To understand the photovoltaic action, we need to consider the situation under illumination. Fig. 2 shows the energy diagram and Fig. 3 the spatial distribution of electron and hole conductivities corresponding to the maximum power point (MPP). At the electron contact on the left, the current is mainly carried by electrons, which, owing to their large conductivity σ_{e} (see Fig. 3), only require a small driving force, the small gradient of their quasi-Fermi energy $\varepsilon_{\mathrm{FC}}$, almost unnoticeable in Fig. 2. Although the holes experience a much larger driving force toward the electron contact on the left, corresponding to a larger gradient in their quasi-Fermi energy $\varepsilon_{\mathrm{FV}}$, their current is smaller than the electron current due to their much smaller conductivity σ_{h}.

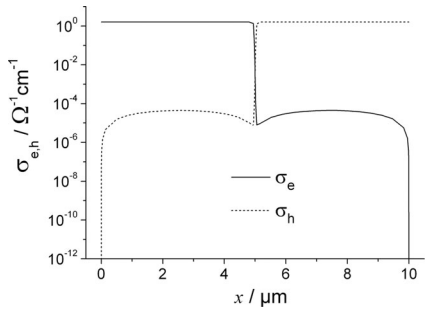

Fig. 3. Spatial distribution of the conductivities of electrons and holes in the p-n homojunction under illumination at the MPP, with $V_{\mathrm{MPP}} = 730$ mV and $J_{\mathrm{MPP}} = 17.1$ mA/cm^2.

Due to the high number of electrons and holes generated by the illumination, the Fermi energy splits up into two quasi-Fermi energies. Thanks to the fact that the driving forces are small for electrons toward the left (the small gradient of $\varepsilon_{\mathrm{FC}}$) and for holes toward the right (the small gradient of $\varepsilon_{\mathrm{FV}}$), most of the difference between the Fermi-energies that exists in the bulk is present as $\varepsilon_{\mathrm{F,left}} - \varepsilon_{\mathrm{F,right}}$ between the two metal contacts. This difference of Fermi-energies defines the voltage V, which

is measurable by a voltmeter:

$$\varepsilon_{\mathrm{F,left}} - \varepsilon_{\mathrm{F,right}} = \mathrm{e}V. \tag{8}$$

The condition of different conductivities for electrons and holes as a requirement for their selective transport toward different contacts is realised in a p-n junction by manipulating the concentrations of electrons and holes by doping. In fulfilling this requirement, the p-n homojunction in this example is, however, far from being ideal, as the concentration of the minority carriers is enhanced by the illumination by a larger factor than that of the majority carriers. The conductivity of the majority carriers is already sufficient in the dark, due to the doping, and changes only slightly upon illumination. The conductivity of the minority carriers at the MPP, however, increases by 12 orders of magnitude (!) when compared with the dark (except for the regions directly adjacent to the contacts) and is too large to prevent the flow of electrons (holes) to the hole (electron) contact.

As a result of the increased hole conductivity, a part of the photogenerated holes flow toward the electron contact where they recombine with electrons. The same happens with a part of the photogenerated electrons at the hole contact due to the increase of their conductivity. This additional recombination reduces both charge current and voltage, resulting in performance values of $J_{\mathrm{SC}} = 17.8\,\mathrm{mA/cm^2}$, $V_{\mathrm{OC}} = 818\,\mathrm{mV}$, $FF = 85.6\%$, and $\eta = 12.5\%$ which are much lower than the ideal values of the Shockley–Queisser model listed in Table I. At the MPP, we find $J_{\mathrm{MPP}} = 17.1\,\mathrm{mA/cm^2}$ and almost all the rest of the photogenerated charge carriers, i.e., corresponding to $17.8\,\mathrm{mA/cm^2}$, do recombine at the electron or hole contact interface.

It is worth mentioning that, considering the key role of carrier conductivities that has been aforementioned, the output of this simple p-n-homojunction solar cell can be improved by reducing the mobilities of both charge carriers. The reason is that in this way the transport of minority carriers toward the wrong contact is reduced, while the conductivity of the majority carriers is still large enough to avoid a noticeable voltage drop. As a consequence, surface recombination losses are lower and the concentration of the minority carriers in the device increases, and with it the open circuit and maximum power voltages. Of course, an extreme reduction of both mobilities would finally deteriorate the device performance due to a nonsufficient conductivity of the majority carriers and the corresponding reduction of the fill factor.

It may seem surprising that the p-n junction in this example has such a low performance when compared with real solar cells, particularly those based on crystalline silicon, which in addition suffer from Auger and defect recombination in the bulk. This is a consequence of the full area metal contacts assumed in this example. If the surface recombination velocity of the minority carriers is reduced, the efficiency increases, and in the case of $v_{\mathrm{sr,min}} \leq 10^{-3}\mathrm{cms}^{-1}$ the simple device of Fig. 1 reaches the Shockley–Queisser limit. However, it is unclear where such an extreme difference for the surface recombination velocities of electrons and holes could originate from in practice.

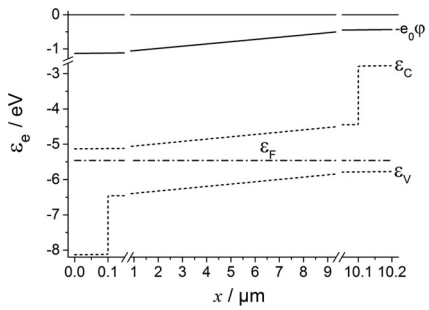

Fig. 4. Energy diagram for the pin-heterojunction with doping densities of $n_{\mathrm{D,A}} = 10^{14}$ cm^{-3} for the wide band-gap selective transport layers in the dark without applied voltage. The "built-in voltage" is $V_{\mathrm{bi}} = 697$ mV. Note the double-interrupted x-axis.

In real solar cells, the contact areas are kept as small as possible, not only for optical reasons but to reduce the rate of surface recombination as well. In addition, in real silicon solar cells, the doping densities close to the contacts are larger than in the bulk, ensuring a better selectivity of the conductivities than in the simple structure of Fig. 1. Device structures where all this is done in an optimized way are among the most efficient silicon solar cells today.

Nevertheless, even in advanced designs of silicon solar cells, there is a considerable number of minority carriers flowing to the "wrong" contact where they are lost by surface recombination [8]–[11]. The awareness of the importance of surface recombination at the metal contacts has led to renewed interest in the development of "passivated contacts" [15]. One of the most successful of such approaches until now is that based on heterojunctions, whose operating principles are discussed in the next example.

B. p-i-n-Heterojunction Solar Cell

A better realization of the principles for implementing a solar cell described by (3) and (4) is to ensure selective transport by using semiconductor materials with a larger band gap and hence a greater potential for vastly different electron and hole conductivities. Fig. 4 shows the energy band diagram in equilibrium of a p-i-n-heterojunction structure with Ohmic contacts. In this structure, an intrinsic absorber is sandwiched between two thin, doped layers with a larger band gap (so-called window layers) that provide selective carrier transport. One layer has a large electron conductivity and a small hole conductivity (see Fig. 6). This electron transport layer allows electrons to flow to the electron contact, while blocking the holes. At the other end of the device, a hole transport layer provides a large hole conductivity and a small electron conductivity. It allows holes to flow to the hole contact, while blocking the electrons. The difference in conductivities is achieved by oppositely doping the thin transport layers, similarly to the idea behind the p-n homojunction. However, the large band gap of the transport layers ensures a smaller conductivity of minority carriers than is possible in the absorber. It is also important that their large band gap makes them transparent to the incident sunlight, which avoids an increase of the minority carrier concentration by illumination. Therefore, in contrast to the simple p-n homojunction discussed

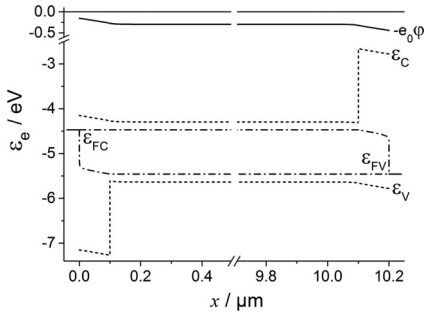

Fig. 5. Energy diagram for the p-i-n heterojunction with doping densities of cm^{-3} for the wide band gap selective transport layers at the MPP with $V_{\mathrm{MPP}} = 987$ mV and $J_{\mathrm{MPP}} = 34.1$ mA/cm^2. Note that the x-axis is interrupted.

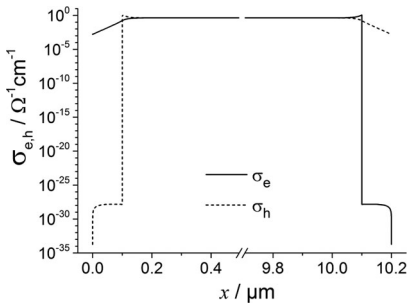

Fig. 6. Conductivity of electrons and holes for the p-i-n heterojunction at the MPP with $V_{\mathrm{MPP}} = 987$mV and $J_{\mathrm{MPP}} = 34.1$ mA/cm^2. Note that the x-axis is interrupted. There is sufficient electron conductivity in almost the entire device ensuring good electron transport and a very strong decrease toward the hole contact located at $x = 10$ μm, which ensures a very low rate of surface recombination (and *vice versa* for the holes).

previously, the small conductivity of the minority carriers in the transport layers is maintained even under illumination.

In the calculations presented below, the selective transport layers have a band gap of $\varepsilon_{\mathrm{G}} = 3\,\mathrm{eV}$, and for the sake of simplicity, no generation of charge carriers in these layers is considered. At the electron contact side, the energies of the conduction band edge of the transport layer and the absorber are equal, while at the hole contact side the valence band edges are aligned. The mobilities of both electrons and holes in the window layers are 100 cm^2/(Vs), the same as in the absorber.

Even for rather low densities of 10^{14} cm^{-3} of donors in the electron transport layer and of acceptors in the hole transport layer, the simulation finds a short-circuit current density of $J_{\mathrm{SC}} = 35.0$ mA/cm^2, an open-circuit voltage of $V_{\mathrm{OC}} = 1082$ mV, a fill factor of $FF = 88.9\%$, and an efficiency of $\eta = 33.7\%$, which is identical to the ideal values from the Shockley–Queisser model.

A comparison between the energy band diagrams in the dark (see Fig. 4) and under illumination (see Fig. 5) shows that the "built-in voltage" of $V_{\mathrm{bi}} = 697$ mV is much smaller than $V_{\mathrm{MPP}} = 987$ mV and $V_{\mathrm{OC}} = 1082$ mV. Hence, at the MPP, there is an electric potential difference of almost 300 mV in the "wrong" direction. This means that the charge carriers move *against* the electric field at MPP without any loss in efficiency, and therefore the reason for charge carrier separation cannot be the presence of an electric field. The real reason for carrier separation and for efficient solar cell operation is that the p-i-n heterojunction ensures a very small minority carrier conductivity in the transport layers even under illumination, so small that surface recombination at the metal contacts is completely avoided.

Fig. 6 shows the corresponding spatial distribution of the conductivities of electrons and holes under illumination at the MPP. As already discussed, the ratio of the conductivities in the selective transport layers is very large due to the large band-gap. In addition, the concentration of minority carriers in these layers is extremely small, not only in the dark but under excitation as well.

It is worth mentioning that for even lower doping levels in the selective transport layers of only 10^9 cm^{-3}, corresponding to a built-in voltage of only 102 mV, the device still reaches the maximum open-circuit voltage. There is, however, a reduction in fill factor, because the conductivity of the majority carriers is too low [12]. With such low conductivities, large gradients of the majority carrier Fermi-energies are required to drive the current resulting in a voltage loss over this majority carrier series resistance. When increasing the mobilities in the selective transport layers (even for both types of carriers) to 2×10^6 cm^2/(Vs), the conductivities of the majority carriers are large enough and the maximum efficiency is reached again. The reason is that due to the large band gap of 3 eV of the selective transport layers and the absence of optical generation in them, the minority carrier concentration is so small that even with this large mobility, their current in the wrong direction remains negligible, hence, the rate of surface recombination at the electrodes. Therefore, it just has to be ensured that the conductivity of the majority carriers is high enough to reach the maximum fill factor.

C. Mobility-Junction Solar Cell

The two preceding cases show that if the necessary differences between electron and hole conductivities in the electron and hole transport layers are achieved by doping, there will always be an electrical potential difference in the dark, the "built-in voltage." Although this "built-in voltage" can be much smaller than the open-circuit voltage, as shown in the previous example of the p-i-n heterojunction, it can never be zero. In order to altogether rule out the electric field as a driving force, we consider a third structure where selective transport is exclusively achieved by a large asymmetry of the carrier mobilities.

Fig. 7 shows the energy band diagram of what could be called a mobility-junction solar cell, where an intrinsic absorber is placed between two thin (0.1 μm) intrinsic layers of the same semiconductor material but with different carrier mobilities. The electron transport layer has a large electron mobility μ_{e} and a much smaller hole mobility μ_{h}. In the hole transport layer, it is the opposite. Neither the selective transport layers nor the absorber are doped; hence, in the dark the concentrations of electrons and holes are the same everywhere, in both selective transport layers and in the absorber; there are no electric fields, and the built-in voltage is $V_{\mathrm{bi}} = 0$.

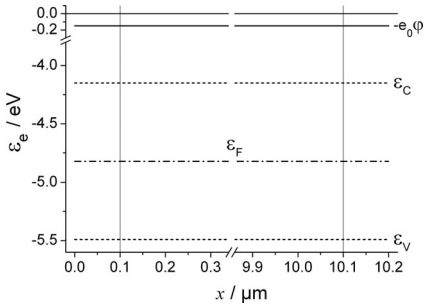

Fig. 7. Energy diagram for the mobility-junction cell (homogeneous concentrations but different mobilities in the thin transport layers) in the dark without applied voltage. There is no built-in electric field as all layers are undoped and have the same band gap and the same electron affinity. The x-axis is interrupted. The electron contact is located at $x = 0$ and the hole contact at $x = 10.2$ μm. The vertical lines at $x = 0.1$ μm and $x = 10.1$ μm are a guide to the eyes and depict the interfaces between absorber and selective transport layers (see text).

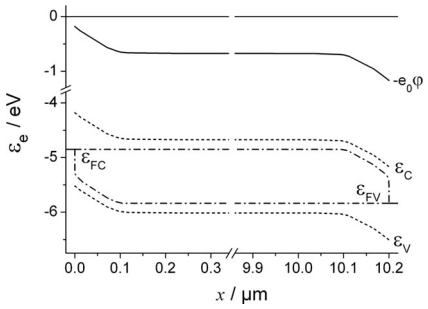

Fig. 8. Energy diagram for the mobility-junction cell at the MPP, with $V_{\mathrm{MPP}} = 987$ mV and $J_{\mathrm{MPP}} = 34.1$ mA/cm^2. The x-axis is interrupted. The electron contact is located at $x = 0$ and the hole contact at $x = 10.2$ μm.

The numerical computer simulations confirm that this structure indeed works as a solar cell. The energy band diagram under illumination and at the MPP is shown in Fig. 8. The conversion efficiency actually reaches the ideal Shockley–Queisser limit if the conductivities are properly chosen. This is achieved by choosing an electron mobility in the electron transport layer as well as a hole mobility in the hole transport layer of 10^8 cm^2/(Vs), while the mobility of holes in the electron transport layer, as well as the mobility of electrons in the hole transport layer, are chosen as 10^{-8} cm^2/(Vs). As a result, there is a large asymmetry between the electron and hole conductivities in the thin layers placed between the absorber and the metal contacts, as shown in Fig. 9. Although such large ratios of electron and hole mobilities are rather unrealistic, we use them to show that this device structure, without doping and without an electric field in the dark, can reach the ideal conversion efficiency, despite a high surface recombination velocity at the metal contacts. The short-circuit current density then is $J_{\mathrm{SC}} = 35$ mA/cm^2, the open-circuit voltage $V_{\mathrm{OC}} = 1082$ mV, the fill factor $FF = 88.9\%$, and the efficiency $\eta = 33.7\%$, which is identical to the ideal limit.

Note that in the previous calculation we neglected light absorption in the thin selective transport layers. If they are assumed to absorb light in the same way as the absorber, the current of the solar cell is reduced by ca. 1.85%, i.e., most of the charge carriers generated in the selective transport layers are lost, as the

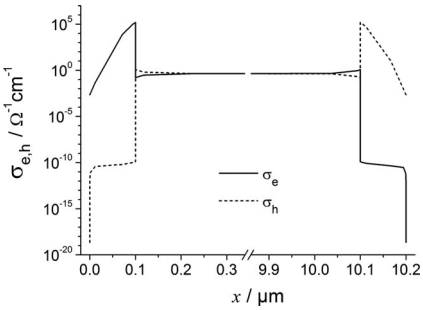

Fig. 9. Conductivity of electrons and holes for the mobility-junction cell at the MPP, with $V_{\mathrm{MPP}} = 987$ mV and $J_{\mathrm{MPP}} = 34.1$ mA/cm^2. Note that the x-axis is interrupted. The decrease of σ_{e} (σ_{h}) toward the electron (hole) contact located at $x = 0$ ($x = 10.2$ μm) is a consequence of the low intrinsic charge carrier density (undoped, ohmic contact).

conductivity of the charge carrier with the very low mobility is extremely low such that most of them recombine in the selective transport layer. A third of those which recombine do this at the surface of electron and hole contact, respectively, and the other two thirds recombine radiatively in the thin transport layers.

The fact that the built-in voltage in equilibrium is $V_{\mathrm{bi}} = 0$, together with a high $V_{\mathrm{MPP}} = 987$ mV, means that at the MPP, there is an electrical potential difference of 987 mV in the "wrong" direction, and the charge carriers move against the corresponding electric field.

The finding that at the MPP the charge carriers have to move *against* the electric field is similar to what was observed in the p-i-n heterojunction, although it is even more extreme in the present case of the mobility-junction structure. In both the cases, the building-up of an electric field in opposition to the direction of the charge carrier movement has the same reason. In both cell structures, the charge carrier densities in the absorber increase strongly under illumination and therefore also in the selective transport layer regions adjacent to the absorber, which can be seen from the separation of the quasi-Fermi levels in Figs. 5 and 8. On the other hand, the majority carrier concentration at the contact interface is rather low, i.e., 10^{14} cm^{-3} for the p-i-n heterojunction and only 1.39×10^8 cm^{-3} in the case of the mobility-junction and does not change under illumination (it is pinned by the assumption of an Ohmic contact, that is, by the Fermi energy of the metal). The result is that there are large gradients of the majority carrier concentration in the selective transport layers. In addition, we have ensured a large conductivity of the majority carriers through doping (p-i-n heterojunction) or through a very high mobility (mobility-junction). As a consequence, the gradients of the quasi-Fermi levels that are required to drive the maximum power current J_{MPP} are very small (and therefore not even visible in Figs. 5 and 8). Therefore, the large gradients in the *chemical* potential of the majority carriers in the transport layers has to be counterbalanced by a gradient of the *electric* potential energy, similar in magnitude but opposite in sign. This is the reason for the electric field being directed opposite to the movement of the charge carriers (it is visible in Figs. 5 and 8 as a bending of the conduction and valence bands near the contacts). An important finding of this study is the fact that, as long as the conductivity of the majority carriers in

the transport layers of the heterojunctions remains sufficiently large, this does not lead to a reduction in fill factor.

At the MPP, a solar cell should have both a high voltage and a high current. High voltage means a large separation of the quasi-Fermi levels, hence, high concentrations of both majority and minority charge carriers. On the other hand, a high current requires highly asymmetric conductivities, which are commonly realized by a low concentration of minority carriers in the vicinity of the contacts. These two contradicting conditions cannot be met easily with a single material that performs the dual function of absorber and transporter, like the simple p-n homojunction in Section IV-A. The superiority of the heterojunctions in Sections IV-B and IV-C is based on a separation of the two functions: they achieve a high concentration of both charge carriers in the absorber while, at the same time, ensuring highly selective transport in the thin layers between absorber and contacts. They work best if there is negligible charge carrier generation in the selective transport layers.

D. Other Solar Cell Constructions

There are, in principle, other ways to realize the necessary selectivity for the charge carriers. One somehow trivial example is to place an intrinsic or lowly doped semiconductor between electrodes with strongly differing work functions. In order to make such a device efficient, it is necessary that the Fermi energy of the electron contact is at higher energies than the bottom of the conduction band of the absorber and the Fermi energy of the hole contact has to be lower than the maximum of the valence band. This way, the work functions lead to electron (hole) accumulation at the electron (hole) contact combined with a depletion of the other kind of charge carrier. The consequence is that the conductivities of electrons and holes differ strongly in the vicinity of the contacts. Of course, there is a strong electric field related to such a large work function difference and in this case it is not possible that the open-circuit voltage exceeds the "built-in" voltage. In real devices, the electric potential distribution (as a consequence of the large difference in work functions of the two contacts) is usually altered due to the presence of surface (gap) states [13], [14]. They can cause a considerable fraction of the potential difference to drop over a very thin dipole layer at the semiconductor/metal interface. This, in turn, leads to a reduced difference between electron and hole concentrations near the contacts which deteriorates the efficiency of such a device.

There is an ongoing research on realizing selective contacts using quantum dot structures placed between the photoactive layer and the metal surface. These structures are, however, much more related to the heterojunction structure, even if a tunneling mechanism is involved.

Ultrathin tunneling layers are also part of selective contact structures being developed for silicon solar cells. Usually their role is to passivate interface defects, while allowing majority carrier transport to a doped semiconductor, such as polysilicon [15] or a conductive metal oxide [16], [17]. The intrinsic amorphous silicon layer present in the most successful type of silicon heterojunction solar cells may also be viewed as a defect-passivating, tunneling layer. Selective carrier tunneling may on its own open new paths to implement selective contacts for solar cells.

V. Conclusion

Three solar cell structures have been examined in detail, two of which work ideally as solar cells, although the electric field at maximum power operating conditions points in the "wrong" direction. All structures adhere to the same operating principle regardless of the existence (and magnitude) of an electric "built-in" field. The driving forces for the movement of electrons and holes are the gradients of their electrochemical potentials, i.e., their quasi-Fermi energies. However, in a solar cell under illumination, these driving forces are not directed "*per se*" to drive electrons and holes toward different terminals. The particle current is proportional to the product of the gradient of the electrochemical potential and the conductivity. This paper has shown that the difference in conductivities of electrons and holes on the way to "their" contact is the decisive condition for selective transport and that this condition has to be maintained even under illumination.

This means that the electrons move—on their way toward the electron contact—through regions with a large electron conductivity, while the current of the holes in that direction is suppressed by a very small hole conductivity, although the force they are subjected to, the gradient of their electrochemical potential, may be much larger than that of the electrons. The opposite happens for holes and electrons on the way toward the hole contact. For the p-n homojunction and the p-i-n heterojunction, different conductivities are achieved by doping. This leads to an electric potential difference, i.e., the so-called "built-in voltage," between the contacts in the dark. Our model calculations prove that this is a side effect resulting from achieving different conductivities for electrons and holes by manipulating their concentrations.

As a direct application of the design principles, we have introduced a "mobility-junction" structure, where different conductivities are achieved by different carrier mobilities and there is no electric potential difference, no "built-in voltage," in the dark. Despite that, this structure reaches the ideal Shockley–Queisser limit. At the MPP, an electric potential difference of 987 mV is produced under illumination and the electrons and holes have to move against the electric field. As a consequence, our examples also show clearly that there is no reason, in principle, that the open-circuit voltage of a solar cell cannot be larger than the "built-in voltage."

Our investigation shows the in principle superiority of a p-i-n heterojunction over a p-n or p-i-n homojunction in achieving selective carrier transport. Note that the absorber in the heterojunction could also be doped (either n- or p-type) without changing the results, as long as radiative recombination is the only loss mechanism in the bulk.

This superiority, however, may be difficult to realize. In our model structures, we have assumed that the interfaces between different materials, such as between the selective transport

layers and the absorber, are not disturbed by interface states, i.e., states with energies within the gap between the conduction band and the valence band, which greatly enhance nonradiative recombination [18]. Exceptions are lattice-matched combinations in the III-V system, where the lattice structure at the interface is disturbed very little. The recent achievement of a new efficiency record for silicon heterojunction solar cells of 25.6% indicates that excellent interface properties can also be obtained between amorphous and crystalline silicon [19], [20]. It is also worth mentioning that advanced homojunction devices incorporating "passivated contacts" can narrow the gap between the two approaches, as demonstrated by the recent report of a 25.0% back contact silicon solar cell [21]. Solar cell technology has advanced enormously in recent years, both in terms of device performance and in the diversity of materials and device structures that have been developed; the general principles and design rules proposed in this paper should enable further scientific progress in the field.

REFERENCES

[1] A. Cuevas and D. Yan, "Misconceptions and misnomers in solar cells," *IEEE J. Photovoltaics*, vol. 3, no. 2, pp. 916–923, Apr. 2013.

[2] P. Würfel, *Physics of Solar Cells*. New York, NY, USA: Wiley, 2009.

[3] ASTM Standard G173, Standard Tables for Reference Solar Spectral Irradiances: Direct Normal and Hemispherical on 37 1 Tilted Surface, ASTM Int. (2014). ASTM Std. G173, Standard Tables for Reference Solar Spectral Irradiances: Direct Normal and Hemispherical on 37 1 Tilted Surface [Online]. Available: http://www.astm.org

[4] *Photovoltaic Devices—Part 3: Measurement Principles for Terrestrial Photovoltaic Solar Devices With Reference Spectral Irradiance Data*, IEC Std. 60904-3,Geneva, Switzerland: http: 2014.

[5] Web site for NREL.'s (2014). NREL AM1.5 Standard Dataset [Online]. Available: http://rredc.nrel.gov/solar/spectra/am1.5/

[6] W. Shockley and H. J. Queisser, "Detailed balance limit of efficiency of p-n junction solar cells", *J. Appl. Phys.*, vol. 32, pp. 510–519, (1961).

[7] Synopsys. (2013). TCAD sentaurus: Sentaurus device user guide, release H-2013.03 [Online]. Available: www.synopsys.com

[8] R. M. Swanson, "Approaching the 29% limit efficiency of silicon solar cells," in *Proc. 31st IEEE Conf. Photovoltaic Sol. Energy Convers.*, Jan. 2005, pp. 889–894.

[9] Z. Hameiri, L. Mai, A. Sproul, and S. R. Wenham, "18.7% efficient laser-doped solar cell on p-type Czochralski silicon", *Appl. Phys. Lett.*, vol. 97, pp. 222111-1–222111-3, 2010.

[10] J. Benick, B. Hoex, M. C. M. Van De Sanden, W. M. M. Kessels, O. Schultz, and S. W. Glunz, "High efficiency n-type Si solar cells on Al2O3-passivated boron emitters," *Appl. Phys. Lett.*, vol. 92, pp. 253504-1–253504-3, (2008).

[11] P. J. Verlinden, M. Aleman, N. Posthuma, J. Fernandez, B. Pawlak, J. Robbelein, M. Debucquoy, K. Van Wichelen, and J. Poortmans, "Simple power-loss analysis method for high-efficiency Interdigitated Back Contact (IBC) silicon solar cells," *Sol. Energy Mater. Sol. Cells*, vol. 106, pp. 37–41, 2012.

[12] U. Rau, G. Kron and J. H. Werner: "Reply to comments on "Electronic Transport in Dye-Sensitized Nanoporous TiO2 Solar Cells Comparison of Electrolyte and Solid-State Devices" On the Photovoltaic Action in pn-Junction and Dye-Sensitized Solar Cells", *J. Phys. Chem. B*, vol. 107, pp. 13547–13550, 2003.

[13] A. M. Cowley and S. M. Sze, "Surface states and barrier height of metal–semiconductor systems", *J. Appl. Phys.*, vol. 36, pp. 3212–3220, 1965.

[14] J. Tersoff, "Schottky barrier heights and the continuum of gap states," *Phys. Rev. Lett.*, vol. 52, pp. 465–468, 1984.

[15] F. Feldmann, M. Bivour, C. Reichel, M. Hermle, and S.W. Glunz, "Passivated rear contacts for high-efficiency n-type Si solar cells providing high interface passivation quality and excellent transport characteristics", *Sol. Energy Mater. Sol. Cells*, vol. 120, part A, pp. 270–274, 2014.

[16] C. Battaglia, S.M. de Nicols, X. Yin, M. Zheng, I. D. Sharp, T. Chen, S. McDonnell, A. Azcatl, C. Carraro, B. Ma, R. Maboudian, R. M. Wallace, and A. Javey, "Hole selective MoOx contact for silicon solar cells," *Nano Lett.*, vol. 14, pp. 967–971, 2014.

[17] C. Battaglia, S. M. De Nicolás, S. De Wolf, X. Yin, M. Zheng, C. Ballif, and A. Javey, "Silicon heterojunction solar cell with passivated hole selective MoO_x contact," *Appl. Phys. Lett.*, vol. 104, pp. 113902-1–113902-5, 2014.

[18] M. Green, *Silicon Solar Cells*. Sydney, Australia: Univ. New South Wales, 1995.

[19] M. Taguchi, A. Yano, S. Tohoda, K. Matsuyama, Y. Nakamura, T. Nishiwaki, K. Fujita, and E. Maruyama, "24.7% record efficiency HIT solar cell on thin silicon wafer," *IEEE J. Photovoltaics*, vol. 4, no. 1, pp. 96–99, Jan. 2014.

[20] http://panasonic.co.jp/corp/news/official.data/data.dir/2014/04/en140410–4/en140410–4.html, 2014.

[21] D. D. Smith, P. Cousins, S. Westerberg, R. De Jesus-Tabajonda, G. Aniero, and Y.-C. Shen, "Toward the practical limits of silicon solar cells," in *Proc. 40th IEEE Photovoltaic Spec. Conf.*, Jun. 2014, pp. 1465–1469.

Uli Würfel received the Ph.D. degree in physics from the University of Freiburg, Freiburg, Germany in 2006.

Since 2009, he has been the Head of the Department "Dye and Organic Solar Cells" with the Fraunhofer Institute for Solar Energy Systems ISE, Freiburg, Germany, and of the group "Organic Solar Cells" with the Freiburg Materials Research Center FMF, the University of Freiburg. His work is mainly dedicated to the characterization and modeling of organic solar cells, their upscaling, and their long-term stability. His current research interests include the general working principles and theoretical modeling of solar cells. He has coauthored 60 scientific articles on solar cells.

Andres Cuevas (SM'96–F'14) received the Ph.D. degree from the Universidad Politecnica de Madrid, Madrid, Spain, in 1980.

He was with Stanford University, Stanford, CA, USA, as a Fulbright Fellow. In 1993, he joined The Australian National University, Canberra, Australia, where he is currently a Professor of engineering. His current research interests include the physics and theoretical modeling of solar cells, the characterization of the fundamental properties of silicon, and the development of carrier-selective, passivated contacts for a new generation of silicon solar cells. He has coauthored 350 scientific articles in the field of photovoltaic solar energy.

Peter Würfel is currently a retired Professor of physics with the University of Karlsruhe, Karlsruhe, Germany, now Karlsruhe Institute of Technology. He has worked on luminescence characterization of solar cells, third-generation methods, and thermodynamic limits of photovoltaic efficiencies. He has published the book Physics of Solar Cells.